

Improvements in Barrier Properties of Poly(lactic acid) Films Coated with Chitosan or Chitosan/Clay Nanocomposite

Seok-Hoon Park,¹ Hyun Soo Lee,² Jae Hoon Choi,² Chang Myeong Jeong,² Myoung Hwan Sung,² Hyun Jin Park^{1,3}

¹College of Life Sciences and Biotechnology, Korea University, Sungbuk-Ku, Seoul 136-701, Republic of Korea

²Research Development Department, Lotte Aluminum, Geumcheon-gu, Seoul 153-010, Republic of Korea

³Department of Packaging Science, Clemson University, Clemson, South Carolina 29634-0320

Received 13 February 2011; accepted 24 October 2011

DOI 10.1002/app.36405

Published online 7 February 2012 in Wiley Online Library (wileyonlinelibrary.com).

ABSTRACT: The feasibility of chitosan or/and clay coatings as an alternative oxygen barrier material to poly(lactic acid) (PLA) film was investigated. The coated films were composed of natural materials based on biodegradable and biocompatible polymers, which exhibit excellent oxygen-barrier properties compared with neat PLA films. Thus, these films can contribute toward effectively reducing environmental pollution. The chitosan/clay nanocomposite solutions were effectively dispersed through the clay using an ultrasonic bath and homogenizer. The barrier and morphology properties of the PLA films were tested by measuring selected film properties such as oxy-

gen transmission rate (OTR), water vapor transmission rate (WVTR), field emission scanning electron microscopy, X-ray diffraction and transmission electron microscope. OTR values measured using the chitosan and chitosan/clay nanocomposite coatings were significantly lower than those measured for neat PLA film. WVTR values measured using chitosan/clay nanocomposite coatings were also lower than those measured for neat PLA film and PLA film coated with chitosan. © 2012 Wiley Periodicals, Inc. *J Appl Polym Sci* 125: E675–E680, 2012

Key words: barrier; clay; coatings; films; morphology

INTRODUCTION

The growth of environmental concerns over synthetic polymers has raised interest in the use of biodegradable alternatives originating from renewable sources. Although biodegradable films are more expensive than petrochemical materials, they will biodegrade into CO₂, water, and biomass under aerobic conditions, or methane and biomass under anaerobic conditions.^{1–3} Based on these characteristics, biodegradable films can contribute toward effectively reducing environmental pollution.

Among the renewable source-based biodegradable plastics, poly(lactic acid) (PLA) is one of the most promising materials since it is thermoplastic, biodegradable, biocompatible and has high-strength, high-modulus, and good processability.⁴ PLA can also be synthesized by condensation polymerization of lactic acid monomers or by the ring opening polymerization of lactide monomers, and these monomers are obtained from the fermentation of renewable sugar

feedstock such as corn or sugar beets.⁵ Because of high-production costs, in the early stages of its development PLA was used in limited areas, such as in the preparation of medical devices (bone surgery, suture, and chemotherapy, etc.). Since production costs have been lowered by new technologies and large-scale production, the application of PLA has now been extended to other commodity areas such as packaging, textiles, and composite materials.⁶ Recently, antimicrobial PLA films were developed by solvent casting methods.⁷ In addition, PLA film can also be made by conventional film extrusion methodology. For these reasons, PLA is an excellent candidate for producing commercial, compostable packaging material. One limitation of PLA is that it is fairly stiff at room temperature. Therefore, a plasticizer is commonly added to promote flexibility.^{8–10} Another major limitation of PLA relative to polyolefin is that it has poor gas barrier properties.¹¹

In this article, a new method was taken where PLA films with poor gas barrier properties were coated with chitosan or chitosan/clay nanocomposite. The coated films were composed of natural materials based on biodegradable and biocompatible polymers, which exhibit excellent oxygen-barrier properties compared with neat PLA films. Thus, these films can contribute toward effectively reducing environmental pollution.

Correspondence to: H. J. Park (hjpark@korea.ac.kr).

Contract grant sponsor: Development of Eco-Packaging Solution Technology; contract grant number: 100031979.

Recently, nanoscale composites of polymers with unmodified clay or modified clay have been studied extensively.^{12–17} The potential improvements include enhanced mechanical strength, weight reduction, increased heat resistance, and improved barrier properties.¹⁸ Montmorillonite (MMT) is the most widely used cationic clay of the smectite group in the generation of polymer nanocomposites. MMT is hydrated alumina-silicate layered clay made up of two silica tetrahedral sheets fused to an edge-shared octahedral sheet of aluminum hydroxide.

Chitosan is a polysaccharide derived from chitin and is mainly composed of 2-amino-2-deoxy- β -D-glucopyranose repeating units and is a polymer based on a renewable material, which exhibits excellent oxygen-barrier properties due to its high crystallinity and hydrogen bonds between the molecular chains.^{19–21} Chitosan and chitin, next to cellulose, are also the second most plentiful natural biopolymers, and are examples of highly basic polysaccharides. Because of this unique property, many potential products using chitosan have been developed, including flocculating agent, chelating agent, additives, adhesives, and coatings.²²

The main objective of this study was to improve the O₂ barrier properties of PLA films coated with chitosan/clay nanocomposite, and to determine some selected properties including oxygen permeability (OP) and water vapor transmission rate (WVTR), as well as assessments by field emission scanning electron microscopy (FESEM), and X-ray diffraction (XRD).

MATERIALS AND METHODS

Materials

The chitosan was purchased from Samsung Chitopia Co. (Siheung, South Korea) and had a degree of deacetylation of 88.8% and a viscosity of 150 cps. The clay, i.e., the organically modified MMT (Cloisite 30B), with a cationic exchange capacity of 90 mequiv/100 g, was supplied by Southern Clay Products (Gonzales, TX). PLA films of 20- μ m thickness were supplied by SKC Co., Ltd. (Suwon, South Korea).

Preparation of PLA films coated with chitosan/clay nanocomposites

A chitosan aqueous solution was prepared by dissolving 2 g of chitosan powder into 100 mL of distilled water containing 1% (v/v) acetic acid. This chitosan solution was mixed with a mechanical stirrer until fully dissolved. Next 40% (by weight) of glycerol was added to the chitosan solution and then glycerol was homogeneously dispersed by vigorous stirring. All samples included glycerol as a

plasticizer because the chitosan coating without glycerol was very brittle (in the case of the chitosan coating only these solutions were used). Then, 1 wt % of clay (vs. chitosan) was added to the chitosan solution with vigorous stirring overnight. These clay suspensions were then treated in an ultrasonic bath for 1 h to expand the gap of clay layers, and clay suspensions were mixed using a magnetic stirrer for 1 h. The mixture was homogenized for 25 min with optimal shear rates (16,000 rpm)

After stirring, PLA films were individually coated with each chitosan or chitosan/clay solution using an automatic film applicator (Yasuda, Japan). The coating speed was 300 mm/s at 60 Hz. The chitosan or chitosan/clay-coated PLA films were dried at ambient conditions for 24 h.

Water vapor transmission rate (WVTR)

The WVTR values of films were measured using a PERMATRAN-W[®] Model 3/61 apparatus (MOCON). Test films were first placed into the six test cells. As the water vapor diffused through the test film, it was carried by carrier gas (N₂) to the detector, and WVTR was continuously recorded. Permatran response was calibrated using a reference film provided by the manufacturer. The tests were performed in triplicate and average mean values were used. Testing was carried out at 38°C under a relative humidity of 100%. WVTR was obtained in g/m² day. All specimens were conditioned at ambient conditions.

Oxygen transmission rate (OTR)

The OTR values of films were measured using an OX-TRAN[®] Model 2/61 apparatus (MOCON, USA). OTR represents the ease with which O₂ traverses films when submitted to a gradient in the partial pressure of O₂ across the films. It is expressed as the quantity (Q) of O₂ molecules passing through a film surface area (A) during time (t) at steady state, under a partial pressure difference (Δp) in O₂ between the two surfaces of the sample:

$$\text{OTR} = Q/A \cdot t \cdot \Delta p \quad (1)$$

Testing was performed at 23°C under an RH of 0%. OTR was measured as cc/m² day transmission rate (WVTR). Measurements were taken three times and the average value was calculated. All specimens were conditioned at ambient conditions.

Haze

Haze is the scattering of light as it passes through a transparent material, resulting in poor visibility

and/or glare. Transmittance measures the amount of light that passes through a sample. Haze and transmission measurements can be useful in product development, process development, and end-use performance testing. Film haze was measured using a Model NDH5000 haze meter (Nippon Denshoku Industries, Japan). The double-beam measurement system utilized a 150-mm integrating sphere with a compensating aperture, applied barium sulfate, and a hatch type trap. The light source was a white light-emitting diode. Triplicate measurements were performed with individually prepared film samples and the average value was calculated.

Field emission scanning electron microscopy

Film surface morphology was measured by FESEM using a MIRA II LM apparatus (Tescan, Czech Republic) operating at 5.0 kV. Images at 3000 \times and 500 \times magnification were acquired.

X-ray diffraction

Wide-angle XRD patterns of the film specimens were recorded using small-angle X-ray scattering. The apparatus was equipped with a General Area Detector Diffraction System (GADDS; Bruker AXS, Germany). The area detector operated at a voltage of 40 kV and a current of 45 mA with CuK α radiation ($\lambda = 0.15406$ nm). The basal spacing of the silicate layer (d_{001}) was calculated using Bragg's Equation (2), allowing calculation of the gap between nano-clay layers:

$$2d \sin \theta = n\lambda, \quad (2)$$

where $n = 1$ and $\lambda = 1.5406$ Å.

Equation (2) can be applied when the XRD angle is small. The parameter definitions are as follows: d is the spacing between the diffracting lattice planes, θ is the measured diffraction angle, n is an integer, and λ is the wavelength of the X-ray radiation used.

Transmission electron microscopy

For transmission electron microscope (TEM) observation, 70-nm sections of the samples were prepared by cutting the sample at room temperature using ultramicrotome at a cutting speed of 0.6 mm/s. The sections were collected in a water-filled trough and placed on 200-mesh copper grids and were cut perpendicular to the surface of the film. The TEM images were taken with a Philips Tecnai 12 TEM at an accelerating voltage of 120.0 kV and the HRTEM images and SAED patterns were taken with a FEI Tecnai 20 TEM equipped with a TVIPS CCD camera at an accelerating voltage of 200.0 kV.

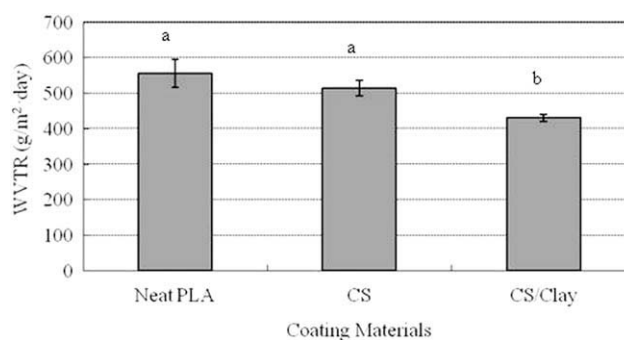


Figure 1 WVTR of neat PLA films, PLA films coated with chitosan, and PLA films coated with chitosan/clay nanocomposite.

Statistical analysis

The OTR, WVTR, and Haze measurements were performed using individually coated films in triplicate, as the replicated experimental units. The significance of each mean property value was determined ($P < 0.05$) by Duncan's multiple range test with SAS software. Each value in a figure is the mean of three replicates with the standard deviation. Any two means in the same figure followed by the same letter are not significantly ($P > 0.05$) different by Duncan's multiple range test.

RESULTS AND DISCUSSION

Water vapor transmission rate (WVTR)

Figure 1 shows the WVTR values of neat PLA films, PLA films coated with chitosan, and PLA films coated with chitosan/clay nanocomposite. The WVTR of the neat PLA films was 556 g/m² day (PLA film thickness : 20 μ m), and the WVTR values of the PLA films coated with chitosan and with chitosan/clay nanocomposite were 515 and 431 g/m² day, respectively (PLA film thickness : 20 μ m, chitosan coating thickness : 2 μ m). Particularly, the WVTR values of PLA films coated with chitosan/clay nanocomposite decreased by 14% compared with the neat PLA films and PLA films coated with chitosan. The decrease in WVTR of the PLA films coated with chitosan/clay nanocomposite is believed to be due to the presence of ordered dispersed nanoparticle layers with large aspect ratios in the polymer matrix.²³ In accordance with this result, the WVTR of polymer/clay nanocomposites can be significantly improved by the incorporation of micro/nanoclay in the film matrix.¹⁴ Furthermore, most hydrophilic natural biopolymers are more compatible with unmodified MMT (Na-MMT), which is hydrophilic. However, organically modified MMT (Cloisite 30B) was used in this research based on previous investigations. Cloisite 30B is a natural

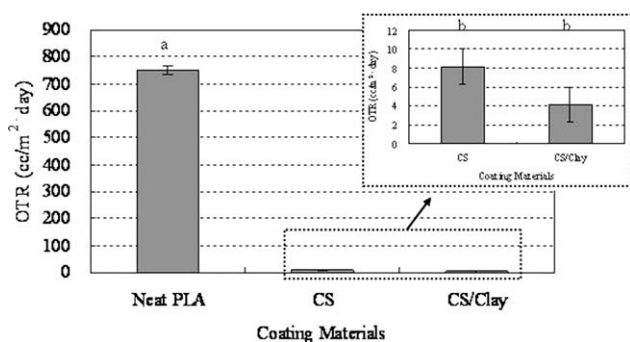


Figure 2 OP of neat PLA films, PLA films coated with chitosan, and PLA films coated with chitosan/clay nanocomposite.

MMT modified with a quaternary ammonium salt. It was shown that Cloisite 30B, which is less hydrophobic than other organically modified MMTs, there is also layer distance increase in interlayer *d*-spacing compared with that of Na-MMT. It was also demonstrated that chitosan/Cloisite 30B nanocomposite exhibited an additional antimicrobial activity due to the quaternary ammonium structure of Cloisite 30B.²⁴

Oxygen transmission rate (OTR)

The OTRs of neat PLA films, PLA films coated with chitosan, and PLA films coated with chitosan/clay nanocomposite are shown in Figure 2. The OP value of the neat PLA films was 736 cc/m² day (PLA film thickness : 20 μm), and the OTR values of the PLA films coated with chitosan and those coated with chitosan/clay nanocomposite were 8 and 4 cc nm/m² day, respectively (PLA film thickness : 20 μm, chitosan coating thickness : 2 μm). In particular, the OTR values of PLA films coated with the chitosan/clay nanocomposite decreased by 99.5% compared with the neat PLA films. This observed decrease in OTR is of great importance in evaluating films for use in food packaging, coatings, and other applications where an efficient polymer barrier is needed. This result also indicates that chitosan and chitosan/

clay nanocomposite coatings on PLA film are eco-friendly materials that can be used as a powerful oxygen barrier. Between the chitosan and the chitosan/clay nanocomposite coatings, OTR values were not significantly different. In the case of polymer/clay nanocomposites, the addition of nanoclay to a pure polymer film improves barrier properties,^{25,26} due to the combination of two phenomena: decreased area available for diffusion due to the replacement of preamble polymer by the impermeable nanoclays, and the increased distance a solute must travel to cross the film as it follows a tortuous path around the impermeable nanoclays.²⁷

Field emission scanning electron microscopy

FESEM images of the PLA films coated with chitosan and those coated with chitosan/clay nanocomposites are shown in Figure 3. In Figure 3(a), the cross-section image of PLA films coated with chitosan shows approximately 2 μm coating thickness. The surface image of PLA films coated with chitosan/clay nanocomposites in Figure 3(b) indicates well dispersed and small size clay particles, which is evidence of the enhanced dispersion of chitosan/clay nanocomposite as achieved by the homogenizer and the sonicator. In this research, the haze properties in Figure 4, and the XRD pattern in Figure 5 indicated that clay particles were intercalated.¹⁴ In the case of polymer/clay nanocomposites, the dispersed phase in nanocomposite membranes becomes more spherical in shape and the size of the domains decrease.²⁸ As the addition of modified clay, the aggregates are small, also confirming that better dispersion of the modified clay and polymer matrix was achieved.²⁹

Haze properties

The haze values of PLA films coated with chitosan were similar to those of the neat PLA films (Fig. 4). However, the haze values of the PLA films coated with chitosan/clay nanocomposite were higher than

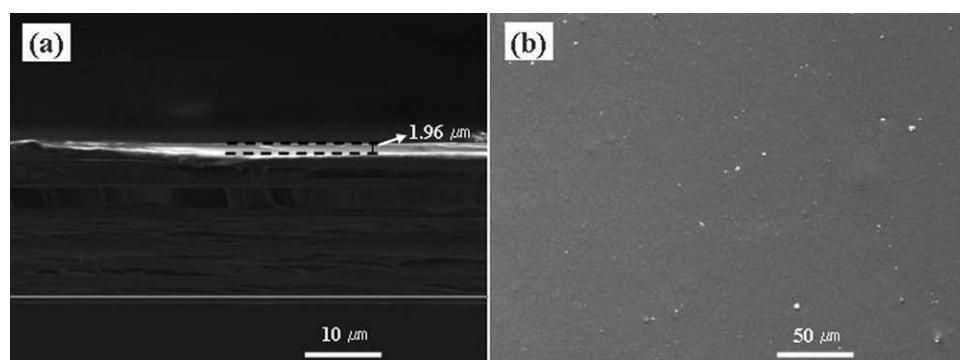


Figure 3 FESEM micrograph of (a) cross-section of PLA films coated with chitosan and (b) surface of PLA films coated with chitosan/clay nanocomposite.

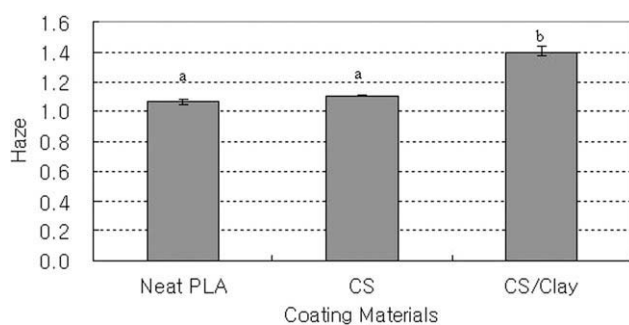


Figure 4 Haze properties of neat PLA films, PLA films coated with chitosan, and PLA films coated with chitosan/clay nanocomposite.

those of the PLA films coated with chitosan, which is consistent with observations of hindered light passage by impermeable nanoclays. Nevertheless, the degree of increase in haze was not markedly changed. In general, the optical properties of well-developed nanocomposite film in polymer/clay nanocomposites are generally not markedly changed when clay platelets with a thickness of about 1 nm are well dispersed through the polymer matrix, since a particle's diameter is less than the wavelength of visible light, and so the passage of light is unhindered.³⁰ However, the large decrease in the transmittance of the composite films indirectly indicates an incomplete dispersion of the clays in the polymer matrix. Also, the transmittance of composite films decreases linearly with increases in clay content.³¹

X-ray diffraction

Clay dispersion within the chitosan was characterized by XRD. Figure 5 shows the XRD patterns of Cloisite 30B powder and PLA films coated with chitosan/clay nanocomposite. The XRD patterns of Cloisite 30B revealed a diffraction peak at $2\theta = 4.89^\circ$, suggesting a layer distance of 1.81 nm. This indicates that there is a 0.62 nm increase in interlayer d -spacing compared with that of Na-MMT (2θ : 7.41° , layer distance: 1.19 nm) due to the replacement of sodium ions with quaternary ammonium cations.³⁰ The peak of the PLA films coated with chitosan/clay nanocomposite was shifted to a lower angle, corresponding to an increase in d -spacing to 6.09 nm (2θ : 1.45°). The higher basal spacing of these PLA films, as compared to clays (tiny shoulder, 2θ : 1.49° , layer distance: 5.92 nm), is attributable to effective dispersion through the use of the homogenizer and sonicator.³¹ The XRD patterns of the PLA films using chitosan-containing clays indicate that the clays can form an intercalated nanostructure. A far more effect way of visualizing nanocomposite morphology is via TEM. In chitosan/clay nanocomposite with a small amount of clay, the reflection peak of the pristine clay disappeared and a tiny

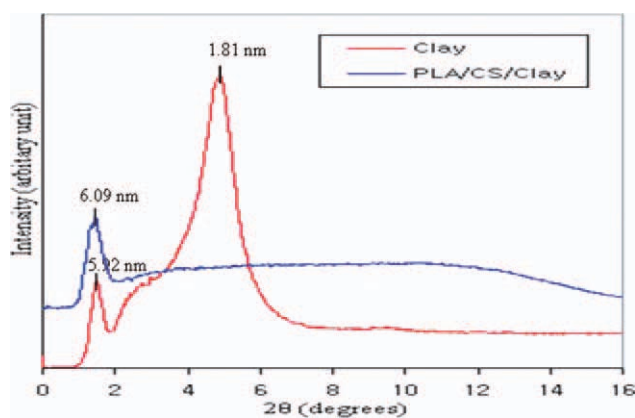


Figure 5 XRD patterns of clay (Cloisite 30B) and PLA films coated with chitosan/clay nanocomposite. [Color figure can be viewed in the online issue, which is available at wileyonlinelibrary.com.]

shoulder appeared at a low angle. This indicates the formation of an exfoliated structure, which is disordered. Because of the hydrophilic and polycationic nature of chitosan in acidic media, chitosan is highly miscible with MMT and can easily intercalate into the interlayers by means of cationic exchange. In addition, the higher basal spacing of clays in polymer/clay composites is due to the intercalation of polymer chains inside the clay layers. The mixed state of intercalated or exfoliated structures can be observed in various weight compositions with modified nanoclay.³²

Transmission electron microscopy

TEM is one of the main tools used for determining the dispersion formation of clay layers.³³ TEM images of the dispersion of clay (Cloisite 30B) within CS/clay nanocomposites are presented in Figure 6.

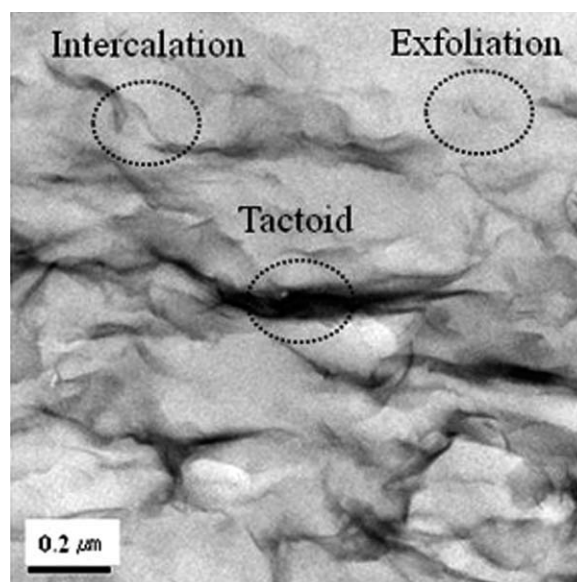


Figure 6 TEM image of PLA film coated with chitosan/clay nanocomposite.

They were well-ordered and dispersed in the chitosan matrix. It was indicated that the interlayer *d*-spacing between nanoclay layers were expanded and that the chitosan/clay nanocomposites were intercalated into the layers of clay. However, although CS/clay nanocomposite was generated with these appropriate processing conditions, perfect exfoliation was not produced and three dispersion types of clay layers such as tactoids, exfoliation, and intercalation were investigated as results of TEM.

CONCLUSION

The use of chitosan/clay nanocomposite coatings improved the water vapor barrier properties of PLA films. This result indicates that the clay particles were effectively dispersed using the homogenizer and sonicator. In particular, the use of chitosan or chitosan/clay nanocomposite coatings significantly improved oxygen barrier properties of the PLA films. This result indicates that chitosan or chitosan/clay nanocomposite coatings on PLA film are eco-friendly materials that can be used as powerful oxygen barriers. Therefore, these increased oxygen and water vapor barrier properties suggest the great potential of PLA films coated with chitosan and chitosan/clay nanocomposite in the application of pharmaceutical and food packaging films.

References

- Weber, C. J.; Haugaard, V.; Festernsen, R.; Bertelsen, G. *Food Additiv Contaminant* 2002, 19, 172.
- Avella, M.; Vlieer, J. J.; Errico, M. E.; Fischer, S.; Vacca, P.; Volpe, M. G. *Food Chem* 2005, 93, 467.
- Howells, D. G.; Henry, B. M. J.; Madocks, H. E. *Assender, Thin Solid Films* 2008, 516, 3081.
- Garlotta, D. *J Appl Polym Environ* 2001, 9, 63.
- Tsuji, H. *Biopolym Med Pharm Appl* 2005, 183.
- Drumright, R. E.; Gruber, P. R.; Henton, D. E. *Adv Mat* 2000, 12, 1841.
- Macheroni, E.; Guillard, V.; Nalin, F.; Mora, L.; Piergiovanni, L. *J Food Eng* 2010, 98, 294.
- Kulinski, S.; Piotrowska, Z. *Polymer* 2005, 46, 10290.
- Pillin, I.; Montrelay, N.; Grohens, Y. *Polymer* 2006, 47, 4676.
- Thellen, C.; Orroth, C.; Froio, D.; Ziegler, D.; Licciarini, J.; Farrell, R.; D'souza, N. A.; Ratto, J. A. *Polymer* 2006, 46, 11716.
- Lehermeier, H. J.; Dorgan, J. R.; Way, J. D. *J Membr Sci* 2001, 190, 243.
- Marian, Z.; Jozef, R. *Polym Test* 2008, 27, 835.
- Bae, H. J.; Park, H. J.; Hong, S. I.; Byun, Y. J.; Darby, D. O.; Kimmel, R. M.; Whiteside, W. S. *LWT* 2009, 42, 1179.
- Casariago, A.; Souza, B. W. S.; Cerqueira, M. A.; Teixeira, J. A.; Cruz, L.; Diaz, R.; Vicente, A. A. *Food Hydrocolloids* 2009, 23, 1895.
- Marcia, R. M.; Fauze, A. A.; Roberto, J. A.; Tara, H. M.; John, M. K.; Luiz, H. M. *J Food Eng* 2009, 92, 448.
- Ebru, G.; Dilay, P.; Cuneyt, H. U.; Oya, A.; Nurfer, G. *Carbohydr Polym* 2007, 67, 358.
- Wu, T. M.; Wu, C. Y. *Polym Degrad Stab* 2006, 91, 2198.
- Ray, S. S.; Okamoto, M. *Progr Polym Sci* 2003, 28, 1539.
- Gallstedt, M.; Tornqvist, J.; Hedenqvist, M. S. *J Polym Sci: Part B* 2001, 39, 985.
- Kittur, F. S.; Haris, K. V.; Udaya, K.; Tharanathan, R. N. *Carbohydr Polym* 2002, 49, 185.
- Wang, S. F.; Shen, L.; Tong, Y. J.; Chen, L.; Phang, I. Y.; Lim, P. Q.; Liu, T. X. *Polym Degrad Stab* 2005, 90, 123.
- Hench, L. L. *Biomaterials* 1998, 19, 1419.
- Yano, K.; Usuki, A.; Okai, A. *J Polym Sci* 1997, 35, 2289.
- Rhim, J. W.; Hong, S. I.; Park, H. M.; Perry, K. W. *J Agri Food Chem* 2006, 54, 5814.
- Lape, N. K.; Nuxoll, E. E.; Cussler, E. L. *J Membr Sci* 2004, 236, 29.
- Garcia, A.; Eceolaza, S.; Iriarte, M.; Uriarte, C.; Etxeberria, A. *J Membr Sci* 2007, 301, 190.
- Cussler, E. L.; Highes, S. E.; Ward, W. J.; Aris, R. *J Membr Sci* 1998, 38, 161.
- Song, L.; Hu, Y.; Wang, S.; Chen, Z.; Fan, W. *J Mater Chem* 2002, 12, 3152.
- Sharma, S. K.; Nayak, S. K. *Polym Degrad Stab* 2009, 94, 132.
- Xu, Y.; Ren, X.; Hanna, M. A. *J Appl Polym Sci* 2006, 99, 1684.
- Rhim, J. W.; Hong, S. I.; Ha, C. S. *LWT* 2009, 42, 612.
- Quang, T. N.; Donald, G. B. *Polymer* 2007, 48, 6923.
- Tang, Y.; Hu, Y.; Song, L.; Zong, R.; Gui, Z.; Chen, Z.; Fan, W. *Polym Degrad Stab* 2003, 82, 127.